Published in final edited form as:
J Hazard Mater. 2014 January 15; 264: . doi:10.1016/j.jhazmat.2013.11.007.

Synergistic adsorption of heavy metal ions and organic pollutants by supramolecular polysaccharide composite materials from cellulose, chitosan and crown ether

Tamutsiwa M. Mututuvari and **Chieu D. Tran***
Department of Chemistry, Marquette University, P.O. Box 1881, Milwaukee, WI 53201, USA

Abstract

We have developed a simple one-step method to synthesize novel supramolecular polysaccharide composites from cellulose (CEL), chitosan (CS) and benzo-15-crown 5 (B15C5). Butylmethylimidazolium chloride [$BMIm^+Cl^-$], an ionic liquid (IL), was used as a sole solvent for dissolution and preparation of the composites. Since majority of [$BMIm^+Cl^-$] used was recovered for reuse, the method is recyclable. The [CEL/CS + B15C5] composites obtained retain properties of their components, namely superior mechanical strength (from CEL), excellent adsorption capability for heavy metal ions and organic pollutants (from B15C5 and CS). More importantly, the [CEL/CS + B15C5] composites exhibit truly supramolecular properties. By itself CS, CEL and B15C5 can effectively adsorb Cd^{2+}, Zn^{2+} and 2,4,5-trichlorophenol. However, adsorption capability of the composite was substantially and synergistically enhanced by adding B15C5 to either CEL and/or CS. That is, the adsorption capacity (q_e values) for Cd^{2+} and Zn^{2+} by [CS + B15C5], [CEL + B15C5] and [CEL + CS + B15C5] composites are much higher than combined q_e values of individual CS, CEL and B15C5 composites. It seems that B15C5 synergistically interact with CS (or CEL) to form more stable complexes with Cd^{2+} (or Zn^{2+}), and as a consequence, the [CS + B15C5] (or the [CEL + B15C5]) composite can adsorb relatively larger amount Cd^{2+} (or Zn^{2+}). Moreover, the pollutants adsorbed on the composites can be quantitatively desorbed to enable the [CS + CEL + B15C5] composites to be reused with similar adsorption efficiency.

Keywords

Supramolecule; Ionic liquid; Adsorption; Heavy metal ions; Endocrine disruptor

1. Introduction

Crown ethers (CRs), with their ability to selectively form complexes with metal ions, have been widely exploited for use in a variety of applications including selective extraction and selective transport of metal ions [1–5]. However, the high cost of CRs, together with difficulty in recycling them, have restricted their use in large-scale process application. The limitations can be alleviated if the CRs are either chemically reacted or grafted onto man-made polymers. It is predicted that CR-based polymers would form stronger complex with better selectivity for metal ions than corresponding crown ethers [6–11]. In fact, CR-based materials synthesized by these methods are reported to exhibit unique features and

*Corresponding author. Tel.: +1 414 288 5428; fax: +1 414 288 7066. chieu.tran@marquette.edu (C.D. Tran)..

Appendix A. Supplementary data Supplementary data associated with this article can be found, in the online version, at http://dx.doi.org/10.1016/j.jhazmat.2013.11.007.

properties, and have been successfully used in a variety of applications including as membranes for extraction of heavy metal ions and for selective ion transport [6–11]. Unfortunately, in spite of their features and properties, practical applications of such CR-based materials are still limited because, in addition to complexity of reactions used in the synthesis which are limited to persons with synthetic expertise, method used may also alter and/or lessen desired properties of CRs [6–11]. It is, therefore, desirable to incorporate CR into a polymer not by grafting or chemical modification with synthetic chemicals and/or polymers but rather by use of naturally occurring biopolymers such as cellulose and/or chitosan.

Cellulose (CEL) and chitosan (CS) are two of the most abundant biorenewable biopolymers on the earth. In these polysaccharides, an extensive network of intra- and inter-hydrogen bonds enables them to adopt a highly ordered structure. While such structure is responsible for CEL to have desirable chemical and mechanical properties and CS to exhibit remarkable properties such as hemostasis, wound healing, bactericide and fungicide, drug delivery and adsorbent for organic and inorganic pollutants, it also makes them insoluble in most solvents [12,13]. This is rather unfortunate because with its superior mechanical and thermal properties, if CEL and CS can be used as a support polymer onto which CR is encapsulated, it will provide a unique means to synthesize CR-based supramolecular composite materials whose properties are a synergistic combination of all of its components, namely, it will have superior mechanical and thermal properties (from CEL), can stop bleeding, heal wound, kill bacteria, deliver drugs (from CS) [14–19] and selectively form complexes with metal ions (from CRs) [6–11]. Unfortunately, to date, such supermolecules have not been realized because of lack of a suitable solvent which can dissolve all three CEL, CS and CRs.

Considerable efforts have been made in the last few years to find inexpensive and “green” solvents which can readily and effectively dissolve CEL and CS [20,21]. Recently, by use of a simple ionic liquid (IL), butyl methylimidazolium chloride ($BMIm^+Cl^-$), a green solvent [22,23], we have successfully found a solution for this problem. Because ($BMIm^+Cl^-$) can dissolve both CEL and CS [24–29], we were able to synthesize [CEL + CS] composites not only without using any acid or base but also were able to keep the biodegradable, biocompatible and anti-infective and drug carrier properties of CS-based materials intact [22,23]. Specifically, the [CEL + CS] composites obtained were found to have superior mechanical strength (from CEL) and excellent antibacterial and adsorption capability for microcystin-LR, a deadly toxin produced by cyanobacteria (from CS) [23]. Furthermore, the composites also inhibit growth of a wider range of bacteria than other CS-based materials prepared by conventional methods; e.g., over a 24 h period, the composites substantially inhibited growth of Methicillin Resistant *Staphylococcus Aureus* (MRSA), Vancomycin Resistant Enterococcus (VRE), *S. aureus* and *Escherichia coli* [22].

The information presented is indeed provocative and clearly indicates that it is possible to use this simple, totally recyclable and one-step process to synthesize novel supramolecular composite materials from CEL, CS and CR. It is expected that the composite materials not only are biocompatible but also may possess all properties of their components, namely mechanical strength (from CEL), excellent adsorbent for pollutants (from CS) and selectively form complexes with metal ions (from CRs). Such considerations prompted us to initiate this study which aims to hasten the breakthrough by using the method which we have developed recently to synthesize novel supramolecular composite materials from CEL, CS and CRs. Results on the synthesis, spectroscopic characterization and applications of the composite materials for removal of heavy metal ions and organic pollutants such as endocrine disruptors are reported herein.

2. Experimental

2.1. Chemicals

Chitosan (MW ≈ 310–375kDa) and cellulose (microcrystalline powder) (Scheme 1) were purchased from Sigma-Aldrich, and used as received. The degree of deacetylation of chitosan, determined by FT-IR method, was found to be (84 ± 2)% [23]. Highly purified water (18 MΩ cm^{-1}) was used to prepare aqueous solutions of zinc(II) nitrate (J.T. Baker), cadmium(II) nitrate and 2,4,5-trichlorophenol (2,4,5-TCP) (Sigma-Aldrich, Milwaukee, WI). Freshly distilled 1-methylimidazole (Alfa Aesar) and 1-chlorobutane (Alfa Aesar, Ward Hill, MA) were used to synthesize 1-butyl-3-methylimidazolium chloride [$BMIm^+Cl^-$] [23]. Benzo-15-crown-5 (B15C5) (Scheme 1), (Alfa Aesar), was used as received.

2.2. Instruments

UV-vis spectra were measured on a Perkin-Elmer Lambda 35 UV/VIS spectrometer. FTIR spectra were measured on a Perkin-Elmer 100 spectrometer at 2 cm^{-1} resolution with either KBr or by a ZnSe single reflection ATR accessory (Pike Miracle ATR). Each spectrum was an average of 64 spectra. X-ray diffraction (XRD) measurements were taken on a Rigaku MiniFlex II diffractometer utilizing the Ni filtered Cu Kα radiation (1.54059 Å). The voltage and current of the X-ray tube were 30 kV and 15 mA respectively. The samples were measured within the 2θ angle range from 2.0 to 40.0°. The scan rate was 5° min^{-1}. Data processing procedures were performed with the Jade 8 program package [30]. Scanning electron microscopic images of surface and cross section of the composite materials were taken under vacuum with an accelerated voltage of 3 kV using Hitachi S4800 scanning electron microscope (SEM). Tensile strength measurements were performed on an Instron 5500R Tensile Tester.

2.3. Preparation of polysaccharide/crown ether composite films

Procedure previously developed in our group for the preparation of [CEL + CS] composite materials was slightly modified to prepare crown ether-based composite materials [22,23]. Essentially, as shown in Scheme 2, a desired amount of crown ether (e.g., 0.60 g of B15C5) was added to 30 g of [$BMIm^+Cl^-$] in a 100-mL 3-neck round bottom flask maintained at 90 °C under argon atmosphere. Under stirring, complete dissolution was achieved in about 30 min. Cellulose (CEL) or chitosan (CS) was then added in portions of 1% weight (with respect to the weight of [$BMIm^+Cl^-$]) each time. Each successive portion was added after the previous one had completely dissolved until the desired amount has been reached. Upon complete dissolution (about 6 h) the homogeneous solutions of crown ether+ polysaccharides in [$BMIm^+Cl^-$] were casted on Mylar sheet to produce thin films with different compositions and concentrations of crown ether, CEL and CS (**Gel Films**). They were then kept at room temperature overnight to allow the solutions to undergo gelation [$BMIm^+Cl^-$] was then removed from the films by washing them in water for about 72 h to yield **Wet Films**. During this period, the washing water was constantly replaced with fresh deionized water to maximize the removal of the ionic liquid. Distillation of the washing aqueous solution renders recovery of [$BMIm^+Cl^-$] for reuse. It was found that at least 88% of the IL used was recovered for reuse. The Wet Films were then either air dried (for mechanical tests) or lyophilized (for adsorption studies and other characterizations) on a Virtis 2 L freeze drier to produce **Dried Films**. It was found that within experimental errors, composite materials prepared using the recovered IL are the same, spectroscopically and adsorptivity, as those made with freshly prepared [$BMIm^+Cl^-$] (Scheme 2).

2.4. Procedure used to measure adsorption of metal ions (Cd^{2+} and Zn^{2+}) by composite

Materials—Metal ion solutions (Cd^{2+} or Zn^{2+}) were prepared separately from analytical grade metal nitrates and the pH of the solutions was adjusted to 6.0 using either 0.2 M HNO_3 or 0.2 M NaOH. Polysaccharide-crown ether composite film (0.2 g) was added to 100 mL of 4.448 mM metal ion solution in a 250 mL Erlenmeyer flask. The mixture was shaken on an orbit shaker (Lab-line 1345R, Barnstead) at 180 rpm under room temperature (25 ± 1 °C) until equilibrium was reached (~24 h for both Cd^{2+} and Zn^{2+}). An aliquot (50 μL for Cd^{2+} and 100 μL for Zn^{2+}) was withdrawn from the flask at predetermined time intervals and diluted with 5% HNO_3. The concentrations of the metal ions were determined using an atomic absorption spectrometer (Perkin-Elmer, AAnalyst 100) at 228.8 nm and 213.9 nm for Cd(II) and Zn(II), respectively [31,32]. The amount of metal ions adsorbed up to each time point was calculated using the following equation:

$$q_t = \frac{(C_i - C_t)\,V}{W} \quad (1)$$

where q_t is the amount of metal ion adsorbed per unit weight of adsorbent (μmol g^{-1}) at time t; C_i and C_t are the concentrations (μmol L^{-1}) of metal ions in the initial solution and at time t respectively; V is the volume (L) of the metal ion solution at time t and W is the dry weight of composite film (g).

2.5. Procedure used to measure adsorption of 2,4,5-TCP by composite materials

The composite films (25.0–28.0 mg) were washed thoroughly in water prior to the adsorption experiments to further insure that [$BMIm^+Cl^-$] was completely removed because the absorption of any residual IL may interfere with that of adsorbates. To wash the composite films, the weighed films were placed in a thin cell fabricated from PTFE whose windows were covered by two PTFE meshes. The meshes ensured free circulation of water through the material during the washing process. The PTFE mold containing the samples was placed in a 2 L beaker which was filled with deionized water and was stirred at room temperature for 60 h. During this time, absorbance of washed water was monitored at 214 and 287 nm to determine the presence of any [$BMIm^+Cl^-$]. The water in the beaker was replaced with fresh de-ionized water every 4 h.

After 60 h, the films were taken out of the water and placed into the sample cuvette. The cell was stirred using a small magnetic spin bar during the measurement. In order to prevent damage to the film by the magnetic spin bar and to maximize the circulation of the solution during measurement, the film was sandwiched between two PTFE meshes. Specifically, a piece of PTFE mesh was placed at the bottom of the spectrophotometric cell. The washed film sample was laid flat on top of the PTFE mesh. Another piece of PTFE mesh was placed on top of the sample and finally the small magnetic spin bar was placed on top of the second mesh. A blank cell which had the same contents as the sample cell but without the composite film was also employed. Exactly 2.70 mL of 390 μM aqueous solution of adsorbate was added to both sample and blank cell. A second blank cell (blank 2) was also employed. This blank cell 2 had the same contents as the sample cell (i.e., PTFE mesh, composite film, PTFT mesh and magnetic spin bar) but without the adsorbate. Any adsorption of the pollutants by the cell content (PTFE mesh, magnetic spin bar) and not by the composite materials was corrected by the signal of blank 1. Blank 2 provided information on any possible interference of absorption of pollutant by leakage of residual IL from the composite film. Measurements were carried out on a Perkin-Elmer Lambda 35 UV/VIS spectrometer set at 289. Measurements were taken at specific intervals (10 min-, 20 min-, 60 min- and 90 min-intervals during the first 60 min, and the next 260 min, 60 min and 90 min, respectively). After each measurement, the cell was returned to a magnetic

stirrer for continuous stirring. Reported values were the difference between the sample signals and those of blank 1 and blank 2. However, it was found that signals measured by both blank cells were negligible within experimental error.

2.6. Analysis of kinetic data

The pseudo-first-order, pseudo-second-order and intra-particle diffusion kinetic models were used to evaluate the adsorption kinetics of Cd^{2+}, Zn^{2+} and 2,4,5-TCP and to quantify the extent of uptake in the adsorption process

Pseudo-first-order kinetic model—The linear form of Lagergren's pseudo-first-order equation is given as [23,33,34]:

$$\ln (q_e - q_t) = \ln q_e - k_1 t \quad (2)$$

where q_t and q_e are the amount of pollutant adsorbed at time t and at equilibrium (μmol g^{-1}) respectively and k_1 (min^{-1} is the pseudo first order rate constant calculated from the slope of the linear plot of ln ($q_e - q_t$) vs. t.

Pseudo-second-order kinetic model—According to the Ho model, the rate of pseudo second order reaction may be dependent on the amount of species on the surface of the sorbent and the amount of species sorbed at equilibrium. The equilibrium sorption capacity, q_e, is dependent on factors such as temperature, initial concentration and the nature of solute-sorbent interactions. The linear expression for the Ho model can be represented as follows [23,33,34]

$$\frac{1}{q_t} = \frac{1}{k_2 q_e^2} + \frac{1}{q_e} t \quad (3)$$

where k_2 is the pseudo-second order rate constant of sorption (g μmol^{-1} min^{-1}), q_e is the amount of analyte adsorbed at equilibrium (μmol g^{-1}), q_t is the amount of analyte adsorbed at any time t (μmol g^{-1}).

If the initial adsorption rate h is

$$h = k_2 {q_e}^2 \quad (4)$$

Then Eq. (3) can be rearranged as

$$\frac{t}{q_t} = \frac{1}{h} + \frac{1}{q_e} t \quad (5)$$

A linear plot can be obtained by plotting t/q_t against t. q_e and h, can be obtained from the slope and intercept; k_2 can be calculated from h and q_e according to Eq. (4).

Detailed information on intraparticle diffusion model can be found in the Supplementary Data.

3. Results and discussion

3.1. Spectroscopic characterization

3.1.1. FT-IR—Encapsulation of crown ethers into the polysaccharide matrices was spectroscopically confirmed by FTIR results. This was achieved by comparing the FTIR spectra of B15C5 powder, regenerated 100% CEL and 100% CS films with their corresponding composite films; i.e., [CEL + B15C5] and [CS + B15C5]. Shown as the pink spectrum in Fig. 1, B15C5 powder, with its benzene ring, exhibits bands characteristics of aromatic C—H groups. Specifically, bands at 3062 cm^{-1}, 1580 cm^{-1}, and 739 cm^{-1} which can be assigned to aromatic C—H stretching, aromatic backbone vibration, and aromatic C—H out-of-plane deformation of ortho-disubstituted benzene, respectively [35]. Since chitosan does not have benzene ring, its spectrum (black curve) contains set of different bands including a broad band at 3500–3200 cm^{-1} which can be assigned to intra- and intermolecular O—H stretch vibration (Fig. 1). Also in this range, at 3500–3400 cm^{-1}, is the primary N-H vibration. Additionally, the bands at 1650 cm^{-1} and 1558 cm^{-1} are those correspond to C=O stretch (amide I) and N—H bending (amide II) respectively [22,23,36,37]. Carefully inspecting spectra of CS-based composite materials with different concentrations of B15C5 reveals that B15C5 was successfully encapsulated into CS. Specifically, not only that the spectrum [CS + B15C5] composite contains bands of both CS and B15C5 but also that intensity of the bands due to aromatic benzene ring in B15C5 increases concomitantly with concentration of B15C5 in the composite. For example, as the concentration of B15C5 increases from 30 to 60% (red and blue spectra), intensity of the bands due to aromatic C—H groups (of B15C5) at ~3062 cm^{-1}, ~1580 cm^{-1} and ~739 cm^{-1} appeared to grow in intensity relatively to other bands due to CS.

Similarly, FTIR results also confirm that B15C5 was successfully encapsulated into the cellulose matrix. Shown as a black spectrum in Fig. SD-1 (Supplementary Information), FTIR spectrum for regenerated 100% CEL exhibits distinct bands attributed to O—H stretching vibrations (3650–3200 cm^{-1}), aliphatic sp^3 C—H stretch (2900 cm^{-1}), C—O—C stretching vibration (1163 cm^{-1}) and C—O stretch at C-3 position (1024 cm^{-1}) [22,23,36–39]. Again, for the [CEL + B15C5] composites, intensity of three bands due to aromatic C-H groups at ~3062 cm^{-1}, ~1580 cm^{-1} and ~739 cm^{-1} grew concomitantly with the concentration of B15C5 in the composites.

3.1.2. UV-visible—Additional evidence on the presence of B15C5 in the [CEL + B15C5] and [CS + B15C5] composite materials was obtained from UV-vis absorption measurements. Shown in Fig. 2 are UV-vis spectra of 100% CS, 100% CEL, 50:50 CS:B15C5, 50:50 CEL:B15C5 and B15C5. As expected, due to its benzene ring, B15C5 exhibits a pronounced absorption band at 278 nm (black curve). Conversely, 100% CEL and 100% CS do not have any absorption in this region (green and red) because they have no UV-vis chromophore. The fact that, similar to B15C5, spectra of both [CEL + B15C5] and [CS + B15C5] composite films also have strong absorption band at 278 nm (green and blue curve) is a clear indication that B15C5 was successfully incorporated into the polysaccharide matrices.

3.1.3. Powder X-ray diffraction (XRD)—Fig. 3 shows XRD spectra for B15C5 powder, regenerated 100% CEL and [CEL + B15C5] composites with different concentrations of B15C5; i.e., from 30% to 50%. B15C5 with its well-defined XRD spectrum seems to indicate that it adopts a highly crystalline structure. Regenerated 100% CEL film exhibits a spectrum with a broad peak at around 20° and a broad shoulder. As illustrated in the figure, the spectrum can be deconvoluted into two bands, a major band at 20.7° and a smaller band at 12.8°. Incorporating B15C5 into CEL leads to change in XRD spectrum. Specifically, not

only both bands shifted toward smaller 2θ value but also the magnitude of the shifts correlates with concentration of B15C5 in the composite. This can be clearly seen when the $2q_{max}$ of both 20.7° and 12.8° band is plotted as a function of B15C5 concentration in the composites (insert in Fig. 3). As illustrated, both 20.7° and 12.8° band shifted to 19.8° and 12.5°, respectively, when 50% of B15C5 was added to the composite. Since B15C5 has a major band at around 8.9°, the results obtained seem to indicate that B15C5 seems to fit relatively well into CEL. B15C5 may induce some change in the structure of the composite compared to that of 100% CEL material. However, the change is relatively minor, and that the structure of [CEL+ B15C5] is more like that of the 100%CEL than of B15C5 powder. Similar results were also obtained for [CS + B15C5] composites (spectra not shown).

3.1.4. Scanning Electron Microscope (SEM)—Analysis of the composite films by SEM reveals some interesting features about the texture and morphology of the materials. Shown in Fig. 4 are surface (four images on left) and cross section images (four images on right) of regenerated one component CS film (top) and CEL film (3rd from top), 50:50 CS:B15C5 composite film (2nd from top) and 50:50 CEL:B15C5 (bottom). As expected, both surface and cross section images clearly indicate that one-component CEL and CS are homogeneous. Chemically, the only difference between CS and CEL is the few —NH_2 groups in the former. However, their structures, as recorded by the SEM, particularly the cross section images, are somewhat different. Specifically, while CS seems to exhibit smooth structure, CEL arranges itself into a fibrous structure. Both composite films (50:50 CS:B15C5 and 50:50 CEL:B15C5) are not only homogeneous but also their morphology is similar to that of CS and CEL, respectively.

3.2. Mechanical properties

As described above, mechanical strengths of CS and crown ether are so poor that, practically, they cannot be used by themselves for applications based on their unique properties. Since CEL is known to have superior mechanical strength, it is expected that adding CEL to these compounds will enable the [CEL + CS] and [CEL + B15C5] composite to have combined properties of its components, i.e., mechanical strength (from CEL) and adsorption of pollutants (from CS and B15C5). Fig. 5 shows plot of tensile strength of [CEL + CS] and [CEL + B15C5] composites as a function of CEL loading in the composites. As expected, it was found that adding CEL into CS substantially increases its tensile strength (Fig. 5). For example, up to 5× increase in tensile strength can be achieved by adding 80% of CEL into CS, and that the tensile strength of the composite material can be adjusted by adding judicious amount of CEL. Similar effect was also found for [CEL + B15C5] composites. That is, adding CEL into B15C5 substantially increase its tensile strength. For example, mechanical strength of B15C5 was so weak that it was not possible to prepare a [CEL + B15C5] composite with less than 50% of CEL. By adding 50% of CEL, a [CEL + B15C5] composite which has a tensile strength of (29 ± 6) MPa can be obtained. Thereafter, it was found that the tensile strength of the composite increases concomitantly with the concentration of CEL, e.g., tensile strengths of composite with 80% and 90% CEL were found to be (47 ± 5) MPa and (54 ± 4) MPa, respectively.

Taken together, XRD, UV–vis, FT-IR and SEM results presented clearly indicate that novel supramolecular polysaccharide composite materials containing CEL, CS and B15C5 were successfully synthesized by use of [$BMIm^+Cl^-$], an IL, as the sole solvent. Since majority (at least 88%) of [$BMIm^+Cl^-$] used was recovered for reuse, the method is recyclable. As anticipated, adding CEL into the composites substantially increases mechanical strength of the composites. It is expected that the composites may also retain properties of CS and B15C5, namely, they would be good adsorbents for organic and inorganic pollutants (from CS and B15C5) and selectively form complexes with different metal ions (from B15C5).

Initial evaluation of their ability to selectively adsorb various metal ions (Cd^{2+} and Zn^{2+}) and endocrine disruptors such as trichlorophenol is described in following section.

3.3. Applications

3.3.1. Adsorption of Cd^{2+}—Experiments were designed to determine: (1) if CEL, CS, [CEL + CS], [CEL + B15C5] and [CS + B15C5] composite materials can adsorb inorganic pollutants (e.g., heavy metal ions including Cd^{2+} and Zn^{2+}) and organic pollutants such as 2,4,5-trichlorophenol (2,4,5-TCP), an endocrine disruptor; (2) if they can, rate constants, adsorbed amounts at equilibrium (q_e) and mechanism of adsorption processes; (3) composite material which gives highest adsorption; and (4) if crown ethers can provide any selectivity on adsorption of metal ions. These were accomplished by initially fitting kinetic data to both pseudo-first order and pseudo-second order models. Appropriate reaction order for the adsorption processes was determined based on correlation coefficients (R^2) and Model Selection Criteria (MSC) values. Rate constants and q_e values were then obtained from the kinetic results [23,33].

Results obtained by pseudo-1st order and pseudo-2nd order fitting of adsorption of heavy metal ions (Cd^{2+} and Zn^{2+}) and 2,4,5-TCP by [CS + CEL], [CS + B15C5] and [CEL + B15C5] composite films are listed in Table SD-1–3 (Supplementary Data). In all cases, the R^2 and the MSC values, are higher for the pseudo-2nd order model than those corresponding for the pseudo-1st order model. The results suggest that the adsorption of Cd^{2+}, Zn^{2+} and 2,4,5-TCP onto [CS + CEL], [CS + B15C5] and [CEL + B15C5] composite films is best described by the pseudo-2nd order model.

Accordingly, pseudo-2nd order kinetic results (equilibrium sorption capacity (q_e) and rate constant (k_2) were then used to evaluate sorption performance of the composite materials. Table 1 lists q_e values for adsorption of Cd^{2+} on CEL, CS, [CEL + CS], [CEL + B15C5], [CS + B15C5] composite films with different compositions (more detailed information including q_e, k, R^2 and MSC values for the adsorption can be found in Table SD I-3 of Supplementary Data). For clarity of presentation and discussion, data from the tables were used to construct a 3D plot of equilibrium adsorption capacity, q_e, as a function of the composition of [CS + B15C5], [CS + CEL] and [CEL + B15C5] composite films with various compositions (Fig. 6). It was found that 1 g of pure chitosan film (i.e., 100% CS) can adsorb up to 104 μmol of Cd^{2+}. Conversely, it was not possible for 100% CEL film to adsorb any of the Cd^{2+} at all. This is as expected because CS, with its amino groups, is known to form complexes with metal ions such as Cd^{2+}. Crown ethers such as B15C5 are often used as extracting reagent for metal ions because they can form stable complexes with metal ions. Experiments were designed to determine if B15C5, when present in solid form as a component of a composite material, can still form complexes and hence, extract Cd^{2+} from solution. Results obtained clearly indicate that properties of B15C5 remain intact when it is part of either CEL-based or CS-based composite materials. For example, [CEL + B15C5] with 20% B15C5 can adsorb up to 179 μmol g^{-1} of Cd^{2+}. This is more than 7× higher than that of [CEL + CS] composite with 20% CS. This is hardly×surprising because compared to CS, B15C5, with its 5 oxygen atoms, can form relatively more stable complexes with Cd^{2+}. At higher B15C5 loading (e.g., 50% and 60%) adsorption capacity of [CEL + B15C5] composites is relatively lower than that of [CEL + CS] composites with comparable CS loading. This is probably due to the fact that mechanical strength (i.e., tensile strength) of the [CEL + B15C5] composites are relatively lower than that of [CEL + CS] composite with comparable CS loading. Of particular interest are results obtained for [CS + B15C5] composites. It is expected, based on results of [CEL + CS] and [CEL + B15C5] composites, that adsorption capability of [CS + B15C5] composites would be much higher than that of [CEL + CS] and [CEL + B15C5] because both CS and B15C5 can extract

Cd^{2+} from solution. However, it was found that the adsorption capacity (q_e value) of the [CS + B15C5] composite is much higher than expected value calculated by adding individual q_e value of CS and B15C5 previously obtained for [CEL + CS] and [CEL + B15C5] composite. For example, q_e value for the 80:20 CS:B15C15 composite was found to be 394 μmol g^{-1} which is much higher than value of 289 μmol g^{-1} calculated by adding 110 μmol g^{-1} found for CS in 20:80 CEL:CS and 179 μmol g^{-1} for B15C5 in 80:20 CEL:B15C5. Similarly, a q_e value of 363 μmol g^{-1} found for 50:50 CS:B15C5 composite is much higher than calculated value of 113.8 μmol g^{-1} (by adding 91 μmol g^{-1} for CS and 22.8 μmol g^{-1} for B15C5). In fact, for all [CS + B15C5] composites, q_e values found are much higher than corresponding calculated values. These results seem to indicate that CS synergistically interact with B15C5 in forming complexes with Cd^{2+} to enable the [CS + B15C5] composite to adsorb relatively higher amounts of Cd^{2+} ions. It is possible that Cd^{2+}, sitting slightly on top of the B15C5 plane, coordinates with 5 oxygen atoms of B15C5 in the bottom, and with nitrogen of the amino group of CS, on top, to form a pseudo-octahedral structure. Such a complex is known to be relatively more stable than complexes formed through five coordination with only B15C5 or with only amino groups of CS. Consequently, higher concentration of such a complex is formed which leads to higher adsorption capacity for Cd^{2+} by [CS + B15C5].

3.3.2. Adsorption of Zn^{2+}—Experiments were also designed to determine if the composite materials can also adsorb other metal ions such as Zn^{2+}. Results obtained, shown in Table 1, seem to indicate that adsorption of Zn^{2+} is much different from that of Cd^{2+} (Again, more detailed information including q_e, k, R^2 and MSC values for the adsorption can be found in Table SD-5 of Supplementary Data). Specifically, pure cellulose film adsorbed more Zn^{2+} than Cd^{2+} whilst, as described above, pure CS film adsorbed more Cd^{2+} than Zn^{2+}. For example, up to 46 μmol g^{-1} of Zn^{2+} can be adsorbed by 100% CEL film whereas hardly any Zn^{2+} can be adsorbed at all by 100% CS film. A 50:50 CEL:B15C5 and a 50:50 CS:B15C5 film can adsorb 233 μmol g^{-1} and 123 μmol g^{-1} of Zn^{2+}, respectively. This could be rationalized by the `hard–soft acid–base' theory. Zinc(II), being a relatively harder acid than cadmium(II), interacts more strongly with oxygen, a hard base, on hydroxyl groups in cellulose. On the other hand, Cd^{2+}, being softer, interacts more strongly with the softer base, nitrogen on glucosamine residues in chitosan. Since B15C5 with its hard base oxygen atoms as the binding sites, can bind to Zn^{2+} more strongly than Cd^{2+} would bind to the same ligand.

Again similar to the adsorption of Cd^{2+} by [CS + B15C5], synergistic effect was also observed for the adsorption of Zn^{2+} as well. Specifically, results seem to indicate that adding either CS or B15C5 to CEL brings more than additive effect on the adsorption of Zn^{2+}, namely, the q_e values of [CEL + CS], [CEL + B15C5] and [CS + B15C5] are more than values calculated by adding q_e value of individual components of the composites. For examples, no Zn^{2+} was adsorbed by 100% CS and only 46 μmol g^{-1} of Zn^{2+} was adsorbed by 100% CEL film whereas up to 233 μmol g^{-1} and 123 μmol g^{-1} of Zn^{2+} were adsorbed by 50:50 CEL:B15C5 and 50:50 CS:15C5, respectively. However, different from the adsorption for Cd^{2+}, the synergistic effect in the adsorption of Zn^{2+} is higher for [CEL + B15C5] than the corresponding for [CS + B15C5]. Again this might also be explained by the hard-soft acid base theory in the formation of more stable pseudo-octahedral complexes between “hard” Zn^{2+} with both oxygen atoms of B15C5 and CEL than with oxygen atoms of B15C5 and “soft” nitrogen atom of amino groups of CS.

Experiments were also performed to investigate effect of pH on adsorption of Cd^{2+} and Zn^{2+}. However, due to the stability of the composite and metal ions, it was not possible to carry out adsorption at all pH's. Specifically, it was found that [CS + B15C5] composite is not stable in acidic condition, and that CS component of the composite dissolved at pH 2.0. Furthermore, cadmium and zinc precipitated at pH 8.5 and 7.6, respectively. Accordingly,

adsorption of Cd^{2+} by [CS + B15C5] was measured at pH 3.9, and pH 1.9 was selected for the adsorption of Zn^{2+} by [CEL + B15C5] (It is noteworthy to add that adsorption of Cd^{2+} and Zn^{2+} at pH 8.0 and 7.1, respectively were also made unsuccessfully because Cd^{2+} and Zn^{2+} solutions were found to be unstable even at these pHs during the measurements). q_e values were found to be (112 ± 6) $\times 10^{-6}$ mol g^{-1} of Cd^{2+} by [CS + B15C5] and (40.6 ± 0.2) $\times 10^{-6}$ mol g^{-1} of Zn^{2+} by [CEL + B15C5]. These values are considerably lower than values listed in Table 1; i.e., (363 ± 10) $\times 10^{-6}$ mol g^{-1} of Cd^{2+} and (233 ± 6) $\times 10^{-6}$ mol g^{-1} of Zn^{2+} which were obtained for 50:50 CS:B15C5 and 50:50 CEL:B15C5 at pH 6.0. Similar observation of relatively lower adsorptivity for metal ions at lower pH was also observed by other groups [8,40–42]. A variety of reasons may account for the lower q_e values. For example, it is known that proton can form complex with crown ether, and the competition between H_3O^+ and Cd^{2+} (or Zn^{2+}) to form complexes with B15C5 is responsible for relatively lower q_e values for Cd^{2+} and Zn^{2+} in acidic condition. Furthermore, while 100% CS can adsorb up to (104 ± 4) $\times 10^{-6}$ mol g^{-1} of Cd^{2+} through complex formation between its amino groups and cadmium at pH 6.0 (Table 1), it was not possible for the CS moiety in 50:50 CS:B15C5 to coordinate with the cadmium ion at pH 3.9 because its amino group has a pK_a value of 6.4, and hence, are almost entirely protonated at this pH.

3.3.3. Adsorption of organic pollutants—As described in the introduction, currently available CS based composite materials, fabricated by either copolymerizing or grafting CS onto man-made polymers, can adsorb organic pollutants such as endocrine disruptors (e.g., polychlorophenols). It is, therefore, important to determine if (1) the [CEL + CS], [CS + B15C5] and [CEL + CS + B15C5] composite materials reported here still retain this unique property and (2) if they do, by adding CS or B15C5, respectively, into the composite, would it have any effect on adsorption of metal ions (Cd^{2+} and Zn^{2+}) by B15C5, and of organic pollutants by CS. Accordingly, experiments were designed to measure adsorption of an endocrine disruptor, 2,4,5-trichlorophenol (2,4,5-TCP), Cd^{2+} and Zn^{2+} by [CEL + CS], [CEL + B15C5], [CS + B15C5] and [CEL + CS + B15C5] composites with different compositions. Results obtained, also listed in Table 1, clearly show that CS is indeed a very good adsorbent for 2,4,5-TCP whereas CEL can hardly adsorb any of this pollutant. For example, 100% CS material can adsorb up to 11.97 × 10^{-3} moL^{-1} Lg^{-1} whereas 100% CEL can adsorb only 2.0 × 10^{-3} moL^{-1} Lg^{-1} of 2,4,5-TCP. Furthermore, adsorption capability (q_e value) of 2,4,5-TCP by [CEL + CS] composite correlates to concentration of CS in the composites (see, for example, q_e values are 5.36 × 10^{-3} moL^{-1} Lg^{-1} and 9.88 × 10^{-3} moL^{-1} Lg^{-1} for [CEL + CS] composites with 20% and 67% CS, respectively). It was also found that B15C5 is not a good adsorbent for this pollutant. This can be seen by the results that q_e value for 50:50 CEL:CS composite is very similar to that for the 20:50:30 CEL:CS:B15C5 composite (9.27 × 10^{-3} moL^{-1} Lg^{-1} and 8.06 × 10^{-3} moL^{-1} Lg^{-1}, respectively). This is because the adsorption is due mainly to CS, and both of these composites have the same 50% concentration of CS. Furthermore, q_e value of 5.36 × 10^{-3} moL^{-1} Lg^{-1} found for 80:20 CEL:CS composite, which contains 20% CS, is similar to the value of 5.95 × 10^{-3} moL^{-1} Lg^{-1} found for the 30:20:50 CEL:CS:B15C5 which also contains 20% CS. These results also indicate that adding B15C5 into the composites does not seem to have any effect on their adsorption for 2,4,5-TCP. This is hardly surprising considering the fact that adsorption of 2,4,5-TCP is known to be due to the amino groups of CS, and since both CEL and B15C5 do not have this group, they are not good adsorbents for this pollutant. More importantly, the results obtained also show that adding CS into the composites does not seem to have any effect on their adsorptivity for Cd^{2+} as well as Zn^{2+}.

Investigations were also carried out to determine if the [CEL + CS + B15C5] composites can be reused after they adsorb 2,4,5-TCP. Typical results obtained for 30:20:50 CEL:CS:B15C5 show that after 24 h, which was long after adsorption equilibrium had been reached, the adsorbed 2,4,5-TCP was completely desorbed from the composite by washing it

with water. Subsequently, measurements were performed to determine if there are any changes in adsorption capability of composites when the composites are reused for the second time, i.e., composites in which previously adsorbed 2,4,5-TCP are desorbed. Shown in Fig. 7 are plot of q_t of adsorption of 2,4,5-TCP as a function of time by 30:20:50 CEL:CS:B15C5 composite films. For comparison, two curves are shown: black curve is for 1st adsorption (i.e., by freshly prepared composite) and red curves is for 2nd adsorption (i.e., adsorption by composite that were regenerated by desorbing 2,4,5-TCP previously adsorbed). As illustrated, adsorption capacity of the composite remains the same after they were regenerated by desorbing 2,4,5-TCP previously adsorbed.

Metal ions (Cd^{2+} or Zn^{2+}) previously adsorbed on the composites were removed by washing the composites with EDTA using a procedure which is modification of methods reported previously [40,43,44]. For example, [50:50 CS:B15C5] composite with Cd^{2+} adsorbed onto it (or [50:50 CEL:B15C5] composite with Zn^{2+} adsorbed onto it) was placed in an Erlenmeyer flask containing 100 mL of 5.0 mM aqueous solution of disodium EDTA, and the flask was shaken on an orbit shaker at 180 rpm at room temperature for 2.0 h. The composite was then removed from the solution, rinsed with distilled water twice, blotted dry, and then was washed with EDTA again using the same procedure for two more time. Readsorption of Cd^{2+} by the [50:50 CS:B15C5] composite (or Zn^{2+} by the [50:50 CEL:B15C5] composite) was then performed using the same procedure as that used in the first time (which was described above in Section 2). It was found that, similar to freshly made composites, the regenerated composites can also effectively adsorb Cd^{2+} and Zn^{2+} at the same adsorption efficiency. q_e value of (380 ± 10) $\times 10^{-6}$ mol g^{-1} of Cd^{2+} was found for the regenerated [50:50 CS:B15C5] composite which is the same within experimental error as the value of (363 ± 10) $\times 10^{-6}$ mol g^{-1} (listed in Table 1) found for the freshly made composite. Similarly, q_e value for adsorption of Zn^{2+} by regenerated [50:50 CEL:B15C5] composite was (267 ± 3) $\times 10^{-6}$ mol g^{-1} which is comparable with the value of (233 ± 6) $\times 10^{-6}$ mol g^{-1}, listed in Table 1, found for the freshly prepared composite.

3.4. Intra-particle pore diffusion

Additional information on mechanism of adsorption process can be gained by analyzing data using the intraparticle diffusion model as described in the Supplementary Data. Fig. 8 shows plots of q_t vs. $t^{1/2}$ for adsorption of Cd^{2+} and Zn^{2+} (A) and 2,4,5-TCP (B) by composite materials with different compositions and concentrations (for clarity, not all but only a few of composites are plotted). It is evident from the plots that there are two separate stages for all three adsorbates and composites. In the first linear portion (Stage I), the adsorbate (Cd^{2+}, Zn^{2+} and 2,4,5-TCP) was rapidly transported from solution through the solution/composite interface and characterized by k_{ip1}. This can be attributed to the immediate utilization of the most readily available adsorbing sites on surfaces of the composites [45–47]. The first stage is followed by a much slower Stage II (second linear portion). In this stage, the adsorbate molecules diffuse into the pores within the particle of the composites and consequently got adsorbed by the interior surface of each particle which is measured by k_{ip2} [45–47]. At this stage, the diffusion resistance increases and causes a decrease in the diffusion rate. With the continuous uptake of the adsorbate from solution the adsorption decrease leading to a lower and lower diffusion rate until the final equilibrium is reached. Table 2 lists values of k_{ip1} and k_{ip2}, for adsorption of Cd^{2+}, Zn^{2+} and 2,4,5-TCP by composite materials with different compositions and concentrations. As expected, it was found that $k_{ip1} > k_{ip2}$ for all adsorbates and all composites. Both k_{ip1} and Zn^{2+} were found to be relatively larger than those for 2,4,5-TCP. This is probably due to the fact that Cd^{2+} and Zn^{2+}, being smaller than 2,4,5-TCP, can diffuse much faster in both solution and in the composites much than 2,4,5-TCP.

4. Conclusions

In summary, we have successfully developed a simple, one-step and recyclable method based on the use of [$BMIm^+Cl^-$], an IL, as a sole solvent to synthesize novel supramolecular polysaccharide composite materials containing CEL, CS and B15C5. The [CEL/CS + B15C5] composites obtained were found to retain properties of their components, namely superior mechanical strength (from CEL), excellent adsorption capability for heavy metal ions and organic pollutants (from B15C5 and CS). More importantly, it was found that the [CEL/CS + B15C5] composites exhibit truly supramolecular properties. Adsorption capability of the composite was substantially and synergistically enhanced by adding B15C5 to either CEL and/or CS. It seems that B15C5 synergistically interact with CS (or CEL) to form more stable pseudo-octahedral complexes between Cd^{2+} (or Zn^{2+}) and oxygen atoms (of B15C5) and nitrogen atoms (of CS) (or oxygen atoms of CEL in the case of Zn^{2+}). As a consequence, the [CS + B15] (or the [CEL + B15C5]) composite can adsorb relatively larger amount Cd^{2+} ions (or Zn^{2+}). Finally, it is noteworthy to add that the pollutants adsorbed on the composites can be quantitatively desorbed to enable the [CS + CEL + B15C5] composite to be reused with similar adsorption efficiency.

Supplementary Material

Refer to Web version on PubMed Central for supplementary material.

Acknowledgments

Research reported in this publication was supported by the National Institute of General Medical Sciences of the National Institutes of Health under Award number R15GM099033.

References

[1]. Katsuhiko, A.; Kunitake, T. Supramolecular Chemistry – Fundamentals and Applications. Springer; Berlin: 2006.

[2]. Rebek J Jr. Molecular behavior in small spaces. Acc. Chem. Res. 2009; 42:1660–1668. [PubMed: 19603810]

[3]. Hinze WL, Armstrong DW. Organized surfactant assemblies in separation science. ACS Symposium Ser. 1987; 342:2–82.

[4]. Fakayode SO, Brady PN, Pollard DA, Mohammed AK, Warner IM. Multicomponent analyses of chiral samples by use of regression analysis of UV-visible spectra of cyclodextrin guest–host complexes. Anal. Bioanal. Chem. 2009; 394:1645–1653. [PubMed: 19484461]

[5]. Khopkar, SM. Analytical Chemistry of Macrocyclic and Supramolecular Compounds. Springer-Verlag; New York: 2002.

[6]. Lamb JD, Nazarenko AY. Selective metal ion sorption and transport using polymer inclusion membranes containing dicyclohexano-18- crown-6. Sep. Sci. Technol. 1997; 32:2749–2764.

[7]. Nazarenko AY, Lamb JD. Selective transport of lead(II) and strontium(II) through a crown etherbased polymer inclusion membrane containing dialkylnaphthalenesulfonic acid. J. Incl. Phenom. Mol. Recogn. Chem. 1997; 29:247–258.

[8]. Yi Y, Wang Y, Liu H. Preparation of new crosslinked chitosan with crown ether and their adsorption for silver ion for antibacterial activities. Carbohydr. Polym. 2003; 53:425–430.

[9]. Gherrou A, Kerdjoudj H, Molinari R, Seta P, Drioli E. Fixed sites plasticized cellulose triacetate membranes containing crown ethers for silver(I), copper(II) and gold(III) ions transport. J. Memb. Sci. 2004; 228:149–157.

[10]. Mohapatra PK, Lakshmi DS, Bhattacharyya A, Manchanda VK. Evaluation of polymer inclusion membranes containing crown ethers for selective cesium separation from nuclear waste solution. J. Hazard. Mater. 2009; 169:472–479. [PubMed: 19398153]

[11]. Yang Z, Wang Y, Tang Y. Synthesis and adsorption properties for metal ions of mesocyclic diamine-grafted chitosan–crown ether. J. Appl. Polym. Sci. 2000; 75:1255–1260.

[12]. Angustine, AV.; Hudson, SM.; Cuculo, JA. Cellulose Sources and Exploitation. Ellis Horwood; New York: 1990.

[13]. Dawsey, TR. Cellulosic Polymers, Blends and Composites. Carl Hanser Verlag; New York: 1994.

[14]. Bordenave N, Grelier S, Coma V. Hydrophobization and antimicrobial activity of chitosan and paper-based packaging material. Biomacromolecules. 2010; 11:88–96. [PubMed: 19994882]

[15]. Rabea EI, Badawy MET, Stevens CV, Smagghe G, Steurbaut W. Chitosan as antimicrobial agent: Applications and mode of action. Biomacromolecules. 2003; 4:1457–1465. [PubMed: 14606868]

[16]. Burkatovskaya M, Tegos GP, Swietlik E, Demidova TN, Castano AP, Hamblin MR. Use of chitosan bandage to prevent fatal infections developing from highly contaminated wounds in mice. Biomaterials. 2006; 27:4157–4164. [PubMed: 16616364]

[17]. Rossi S, Sandri G, Ferrari F, Benferonic MC, Caramella C. Buccal delivery of acyclovir from films based on chitosan and polyacrylic acid. Pharm. Dev. Technol. 2003; 8:199–208. [PubMed: 12760570]

[18]. Jain D, Banerjee R. Comparison of ciprofloxacin hydrochloride-loaded protein, lipid, and chitosan nanoparticles for drug delivery. J. Biomed. Mater. Res. B Appl. Biomater. 2008; 86:105–112. [PubMed: 18098198]

[19]. Ngah WSW, Isa IM. Comparison study of copper ion adsorption on chitosan, Dowex A-1, and Zerolit 225. J. Appl. Polym. Sci. 1998; 67:1067–1070.

[20]. Cai J, Liu Y, Zhang L. Dilute solution properties of cellulose in LiOH/urea aqueous system. J. Polym. Sci. B Polym. Phys. 2006; 44:3093–3101.

[21]. Fink HP, Weigel P, Purz HJ, Ganster J. Structure formation of regenerated cellulose materials from NMMO-solutions. Progress Polym. Sci. 2001; 26:1473–1524.

[22]. Tran CD, Duri S, Harkins AL. Recyclable synthesis, characterization, and antimicrobial activity of chitosan-based polysaccharide composite materials. J. Biomed. Mater. Res. Part A. 2013; 101A:2248–2257.

[23]. Tran CD, Duri S, Delneri A, Franko M. Chitosan-cellulose composite materials: preparation, characterization and application for removal of microcystin. J. Hazard. Mater. 2013; 252–253:355–366.

[24]. Han X, Armstrong DW. Ionic liquids in separations. Acc. Chem. Res. 2007; 40:1079–1086. [PubMed: 17910515]

[25]. Wasserscheid, P.; Welton, T. Ionic Liquids in Synthesis. Wiley-VCH; Weinheim: 2003.

[26]. Swatloski RP, Spear S, Holbrey JD, Rogers RD. Dissolution of cellulose in ionic liquids. J. Am. Chem. Soc. 2002; 124:4974–4975. [PubMed: 11982358]

[27]. Tran CD, Lacerda SHP. Determination of binding constants of cyclodextrins in room temperature ionic liquids by near-infrared spectrometry. Anal. Chem. 2002; 74:5337–5341. [PubMed: 12403590]

[28]. El Seould OA, Koschella A, Fidale LC, Dorn C, Heinze T. Applications of ionic liquids in carbohydrate chemistry: a window of opportunities. Biomacro-molecules. 2007; 8:2629–2647.

[29]. Mora-Pale M, Meli L, Doherty TV, Linhardt RJ. Room temperature ionic liquids as emerging solvents for the pretreatment of lignocellulosic biomass. Biotechnol. Bioeng. 2011; 108:1229–1245. [PubMed: 21337342]

[30]. Duri S, Majoni S, Hossenlopp JM, Tran CD. Determination of chemical homogeneity of fire retardant polymeric nanocomposite materials by near-infrared multispectral imaging microscopy. Anal. Lett. 2010; 43:1780–1789.

[31]. Asencios YJO, Sun-Kou MR. Syntheis of high-surface-area γ-Al_2O_3 from aluminum scrap and its use for the adsorption of metals: Pb(II), Cd(II) and Zn(II). Appl. Surf. Sci. 2012; 258:10002–10011.

[32]. Monier M, Abdel-Latif DA. Preparation of cross-linked magnetic chitosan-phenylthiourea resin for adsorption of Hg(II), Cd(II) and Zn(II) ions from aqueous solutions. J. Hazard. Mater. 2012; 209–210:240–249.

[33]. Chakraborty S, Chowdhury S, Saha PD. Adsorption of crystal violet from aqueous solution onto NaOH-modified rice husk. Carbohydr. Polym. 2011; 86:1533–1541.

[34]. Ho YW, McKay G. The kinetics of sorption of divalent metal ions onto sphagnum moss peat. Water Res. 2000; 34:735–742.

[35]. Saleh MI, Kusrini E, Salhin A, Adnan R, Rahman IA, Saad B. Structure and; thermal stability of the benzo-15-crown-5 with lanthanum(III) bromide complex. Indones. J. Chem. 2004; 4:139–144.

[36]. Khan A, Khan RA, Salmieri S, Tien CL, Riedl B, Bouchard J, Chauve G, Tan V, Kamal MR, Lacroix M. Mechanical and barrier properties of nanocrystalline cellulose reinforced chitosan based nanocomposite films. Carbohydr. Polym. 2012; 90:1601–1608. [PubMed: 22944422]

[37]. Leceta I, Guerrero P, Caba KDL. Functional properties of chitosan-based films. Carbohydr. Polym. 2013; 93:339–346. [PubMed: 23465939]

[38]. Huq T, Salmieri S, Khan A, Khan RA, Tien CL, Riedl B, Fraschini C, Bouchard J, Uribe-Calderon J, Kamal MR, Lacroix M. Nanocrystalline cellulose (NCC) reinforced alginate based biodegradable nanocomposite film. Carbohydr. Polym. 2012; 90:1757–1763. [PubMed: 22944444]

[39]. Rochester CH, Stratchan A. The adsorption of benzo-15-crown-5 ether from water onto carbon surfaces. J.Colloid Interface Sci. 1996; 177:339–342.

[40]. Ngah WSW, Endud CS, Mayanar R. Removal of copper(II) ions from aqueous solution onto chitosan and cross-linked chitosan beads. React. Funct. Polym. 2002; 50:181–190.

[41]. Juang R, Shao H. Effect of competitive adsorption of Cu(II), Ni(II), and Zn(II) from water onto chitosan beads. Adsorption. 2002; 8:71–78.

[42]. Ngah WSW, Ghani SA, Kamari A. Adsorption behavior of Fe(II) and Fe(III) ions in aquesous solution on chitosan and cross-linked chitosan beads. Bioresour. Technol. 2005; 96:443–450. [PubMed: 15491825]

[43]. Zou Z, Qiu R, Zhang W, Dong H, Zhao Z, Zhang T, Wei X, Cai X. The study of operating variables in soil washing with EDTA. Environ. Pollut. 2009; 157:229–236. [PubMed: 18774633]

[44]. Tsang SW, Lo IMC, Chan KL. Modeling the transport of metals with rate limited EDTA-promoted extraction and dissolution during EDTA-flushing of copper-containing soils. Environ. Sci. Technol. 2007; 41:3660–3666. [PubMed: 17547193]

[45]. Weber JW, Morris JC. Kinetics of adsorption of carbon from solution. J. Sanit. Eng. Div., Am. Soc. Civ. Eng. 1963; 89:31–39.

[46]. Hameed BH, Chin LH, Rengaraj S. Adsorption of 4-chlorophenol onto activated carbon prepared from rattan sawdust. Desalination. 2008; 225:185–198.

[47]. Elsherbiny AB, Salem MA, Ismail AA. Influence of alkyl chain length of cyanine dyes on adsorption by Na^{+}-montmorillonite from aqueous solutions. Chem. Eng. J. 2012; 200:283–290.

HIGHLIGHTS

- A novel and recyclable synthetic method using an ionic liquid, a green solvent.
- Composites synthesized from cellulose (CEL), chitosan (CS) and crown ether (B15C5).
- [CEL/CS + B15C5] retain properties of individual components.
- Synergy between B15C5 and either CEL or CS enhanced adsorption of Cd^{2+}.
- [CEL/CS + B15C5] exhibits truly supramolecular properties.

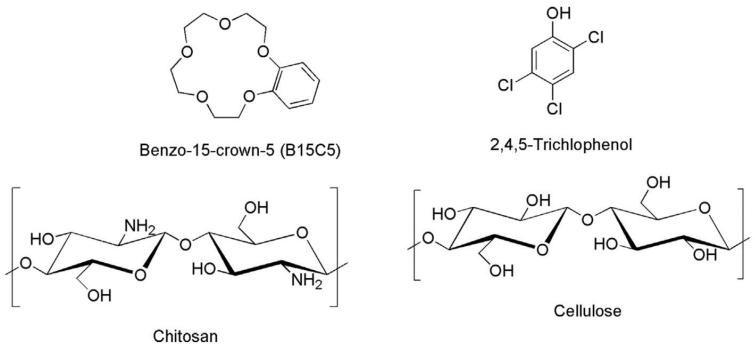

Scheme 1.
Compounds used in this study.

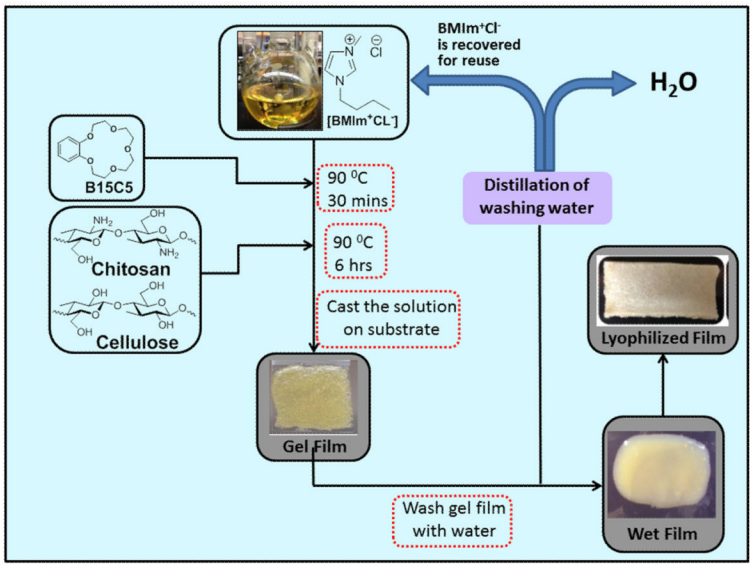

Scheme 2.
Procedure used to prepare the [CEL/CS + B15C5] composites.

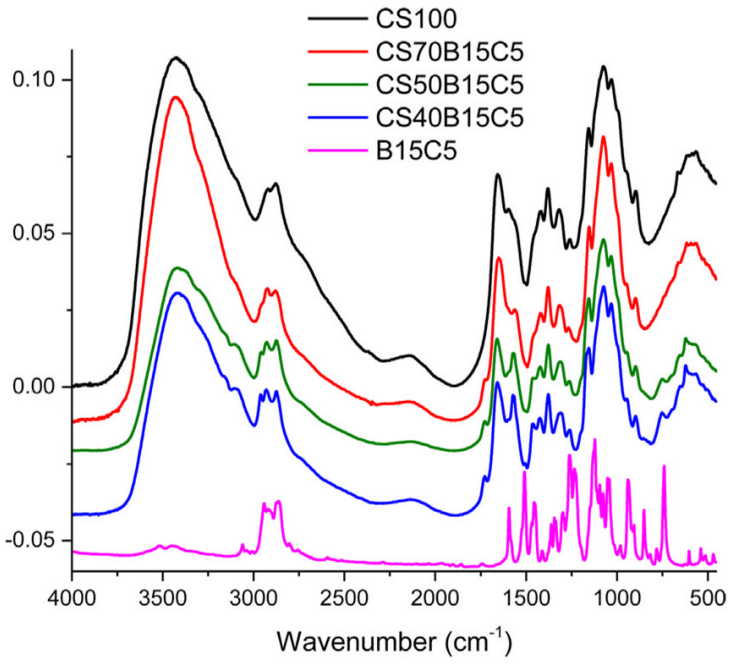

Fig. 1.

FTIR spectra of benzo-15-crown-5 powder (B15C5) (pink), 100% CS (black), 70:30 CS:B15C5 (red), 50:50 CS:B15C5 (green) and 40:60 CS:B15C5 (blue). (For interpretation of the references to color in figure legend, the reader is referred to the web version of the article.)

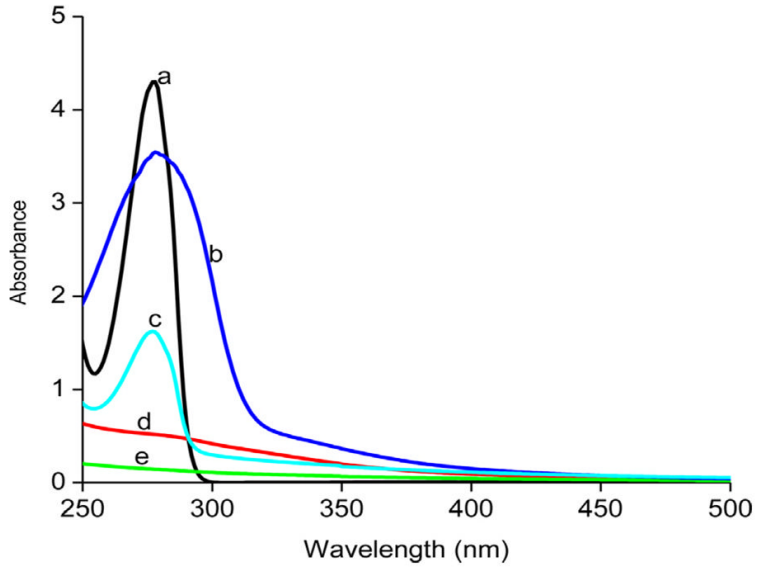

Fig. 2.

UV-vis absorption spectra of B15C5 (a), 50:50 CS:B15C5 (b), 50:50. CEL:B15C5 (c), 100% CS (d), and 100% CEL (e) and X10^{-4}M of B15C5 in chloroform.

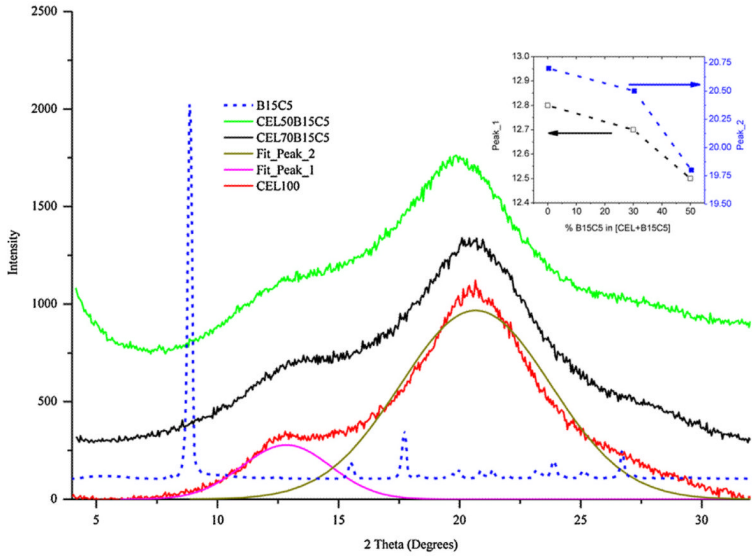

Fig. 3.

XRD spectra of B15C5 powder (blue dashed line), 100% CEL film (red), 50:50. CEL:B15C5 film (green) and 70:30 CEL:B15C5 film (black). Insert is plot of $2\theta_{max}$ value for resolved band at 12.8° and 20.7° as a function of B15C5 concentration in the composites. (For interpretation of the references to color in figure legend, the reader is referred to the web version of the article.)

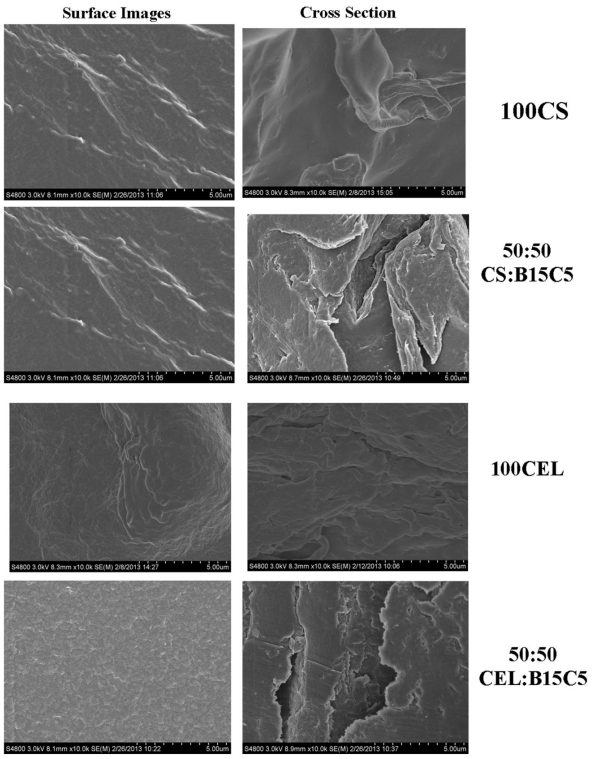

Fig. 4.
SEM images of surface (left images) and cross section (right images) of regenerated films of 100% CS (top row), 50:50 CS:B15C5 (2nd row), 100% CEL (third row) and 50:50 CEL:B15C5 (bottom row).

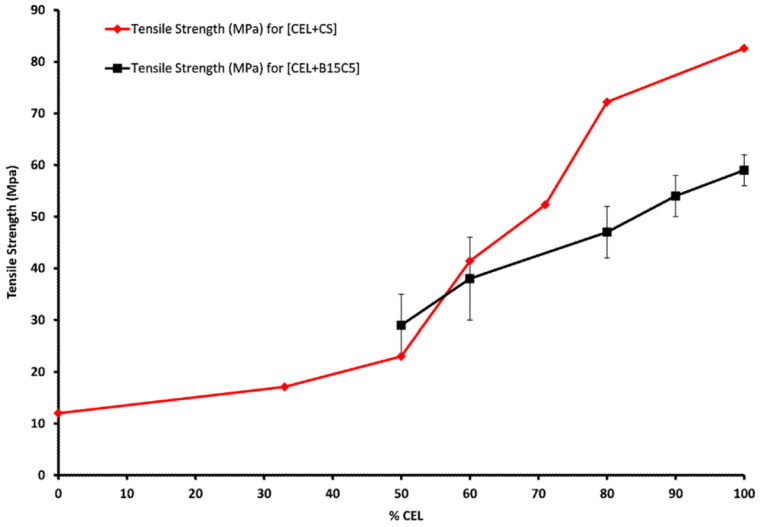

Fig. 5.
Plots of tensile strength as a function of CEL concentration in [CEL+CS] composites (red curve) and [CEL+B15C5] composites (black curve).

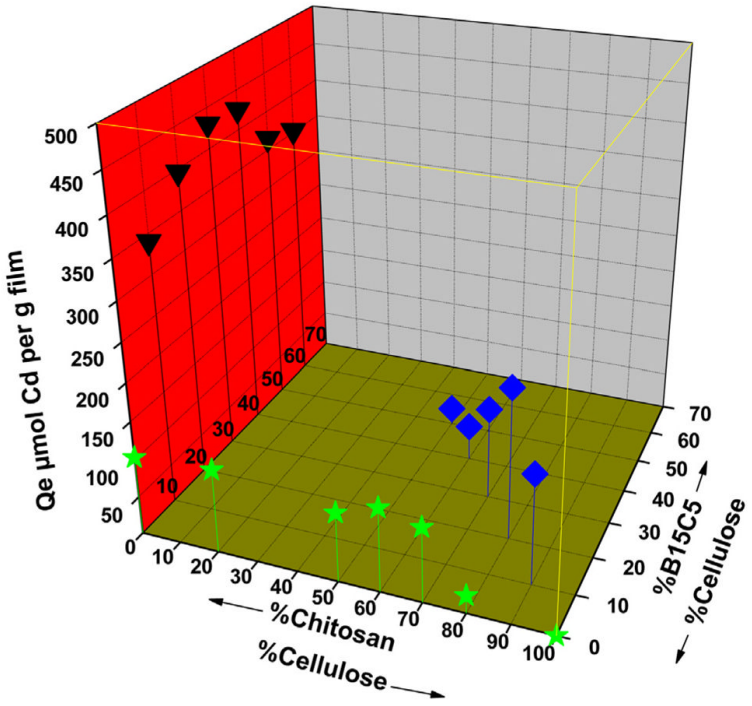

Fig. 6.

3D plot of amount of Cd^{2+} adsorbed at equilibrium (q_e) as a function of CEL, CS and B15C5 concentration in the [CEL + CS], [CEL + B15C5] and [CS + B15C5] composites. See text for detailed information.

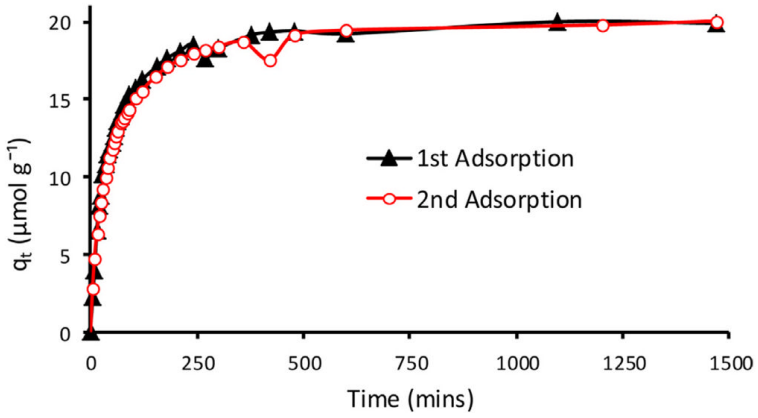

Fig. 7.

Plot of q_t of adsorption of 2,4,5-TCP as a function of time by 30:20:50 CEL:CS:B15C5 composite film: Black curve is for 1st adsorption (i.e., by freshly prepared films) and red curve is for 2nd adsorption (i.e., adsorption by films that were regenerated by desorbing 2,4,5-TCP previously adsorbed). (For interpretation of the references to color in figure legend, the reader is referred to the web version of the article.)

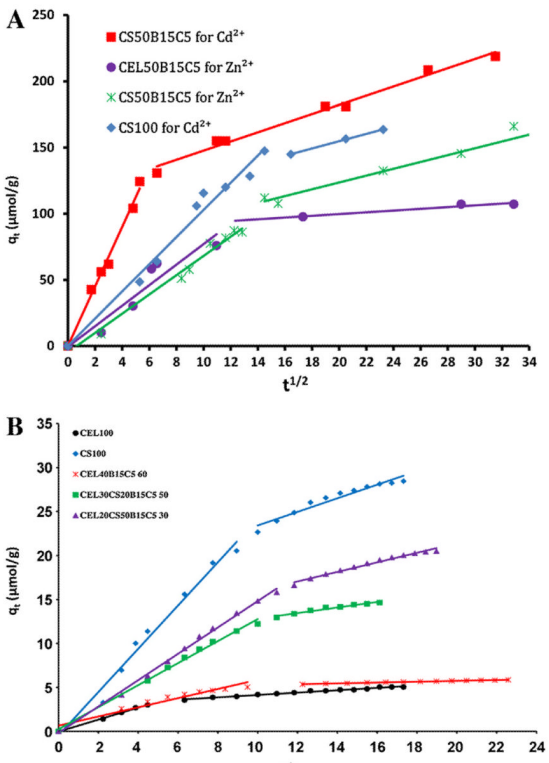

Fig. 8.

Intra-particle diffusion plots for adsorption of (A) Cd^{2+} and Zn^{2+} and (B) 2,4,5-trichlorophenol by composite materials.

Table 1

Equilibrium sorption capacity (q_e) value for Cd^{2+}, Zn^{2+} and 2,4,5-trichlorophenol by [CEL + CS], [CEL + B15C5] and [CS + B15C5] composite materials.

Cellulose	Chitosan	B15C5	2,4,5-TCP $q_e \times 10^6$, mol g^{-1}	Cadmium $q_e \times 10^6$, mol g^{-1}	Zinc $q_e \times 10^6$, mol g^{-1}
100			5.40 ± 0.08		46 ± 1
80	20		14.34 ± 0.03	23.0 ± 0.2	
71	29		15.09 ± 0.02	98 ± 3	
60	40		21.68 ± 0.06	110 ± 10	
50	50		24.76 ± 0.07	91 ± 4	178 ± 4
30	70				186 ± 3
20	80			110 ± 6	
33	67		27.0 ± 0.2		
40		60	5.97 ± 0.03		
70	30				
	100		32.3 ± 0.2	104 ± 4	Not detectable
90		10		142 ± 4	
80		20		179 ± 7	75 ± 2
70		30		115 ± 5	
60		40		48 ± 1	
50		50		22.8 ± 0.2	233 ± 6
	90	10		345 ± 10	
	80	20		394 ± 7	
	70	30		423 ± 20	157 ± 5
	60	40		436 ± 10	
	50	50		363 ± 10	123 ± 3
	40	60		333 ± 10	190 ± 9
30	20	50	16.1 ± 0.1	250 ± 4	
20	50	30	23.75 ± 0.09	245 ± 4	
35	35	30		342 ± 8	
50	20	30		161 ± 2	

Table 2

Intra-particle diffusion rate constants for adsorption of Cd^{2+}, Zn^{2+} and 2,4,5-trichlorophenol by composite materials intra-particle diffusion rate constants for Cd^{2+} and Zn^{2+} adsorption.

Intra-particle diffusion rate constants for Cd^{2+} and Zn^{2+} adsorption

Cellulose	Chitosan	B15C5	Metal ion adsorbed	k_{ip1} (μmol g^{-1} $min^{-1/2}$)	k_{ip2} (μmol g^{-1} $min^{-1/2}$)
	50	50	Cd^{2+}	22 ± 1	3.4 ± 0.2
	100		Cd^{2+}	10.3 ± 0.6	2.7 ± 0.9
	50	50	Zn^{2+}	7.3 ± 0.4	2.6 ± 0.3
50		50	Zn^{2+}	8 ± 1	0.7 ± 0.2

Intra-particle diffusion rate constants for 2,4,5-trichlorophenol adsorption

Cellulose	Chitosan	B15C5	k_{ip1} (μmol g^{-1} $min^{-1/2}$)	k_{ip2} (μmol g^{-1} $min^{-1/2}$)
	100		2.5 ± 0.1	0.77 ± 0.06
100			0.68 ± 0.02	0.135 ± 0.005
40		60	0.52 ± 0.05	0.049 ± 0.001
30	20	50	1.25 ± 0.04	0.32 ± 0.03
20	50	30	1.50 ± 0.03	0.54 ± 0.02